Computing (2010) 88:173–191
DOI 10.1007/s00607-010-0092-1

Use of a double Fourier series for three-dimensional shape representation

Artemy Baxansky · Nahum Kiryati

Received: 16 April 2010 / Accepted: 3 May 2010 / Published online: 21 May 2010

Abstract The representation of three-dimensional star-shaped objects by the double Fourier series (DFS) coefficients of their boundary function is considered. An analogue of the convolution theorem for a DFS on a sphere is developed. It is then used to calculate the moments of an object directly from the DFS coefficients, without an intermediate reconstruction step. The complexity of computing the moments from the DFS coefficients is $O(N^2 \log N)$, where N is the maximum order of coefficients retained in the expansion, while the complexity of computing the moments from the spherical harmonic representation is $O(N^2 \log^2 N)$. It is shown that under sufficient conditions, the moments and surface area corresponding to the truncated DFS converge to the true moments and area of an object. A new kind of DFS—the double Fourier sine series—is proposed which has better convergence properties than the previously used kinds and spherical harmonics in the case of objects with a sharp point above the pole of the spherical domain.

Keywords Fourier series on spheres · Three-dimensional shape analysis · Star-shaped objects · Moments

Mathematics Subject Classification (2000) 42B05 · 33C55 · 65T40

Communicated by D. Saupe.

A. Baxansky (✉)
Zoran Microelectronics Ltd., Advanced Technology Center,
P.O. Box 15015, 31905 Haifa, Israel
e-mail: artemy.baxansky@gmail.com

N. Kiryati
School of Electrical Engineering, Tel Aviv University,
69978 Tel Aviv, Israel
e-mail: nk@eng.tau.ac.il

1 Introduction

It is well-known that spherical harmonics can be an accurate and efficient way to represent three-dimensional (3D) shapes [3,8]. Consider a star-shaped object whose surface is described in spherical coordinates by a boundary function $r = r(\theta, \phi)$. The function $r(\theta, \phi)$ can be expanded in the basis of spherical harmonics. While the spherical harmonic representation possesses many desirable properties, such as good energy compaction and rotation invariance, the computational complexity of the transformation from the spatial domain to the spherical harmonic coefficients and vice versa can be considered as a drawback in some cases. The relatively high computational complexity is attributed to the associated Legendre functions used in the latitudinal direction, which are not amenable to the fast Fourier transform (FFT). A straightforward evaluation of the spherical harmonic transform (SHT) requires $O(N^3)$ operations, where N is the maximum order of coefficients retained in the expansion. With the use of the fast SHT [7,9], the complexity is reduced to $O(N^2 \log^2 N)$. As is well-known, for a function defined on the Cartesian plane, the transformation between the spatial and the Fourier domains can be done by means of the 2D FFT with a complexity of $O(N^2 \log N)$, where N is the maximum order of the Fourier coefficients. Therefore, for the same maximum order of frequency-domain coefficients, the complexity of the transformation between the spatial and the frequency domains for the spherical harmonic representation is higher by a factor of $\log N$ than in Cartesian geometry.

In 1974, Orszag [12] proposed an alternative expansion for problems in spherical geometry, called Fourier series on spheres, or double Fourier series (DFS). In the DFS representation, for each azimuthal number m, a function is expanded in the latitudinal direction in a sine or a cosine Fourier series, possibly multiplied by $\sin^s \theta$, where s is an integer depending on m. The advantage of a DFS is that the transformation from the spatial domain to the DFS coefficients and back can be performed using the FFT, so the DFS representation is computationally simpler than the spherical harmonic one.

A DFS has been used for solving partial differential equations (PDEs) on the unit sphere by spectral and pseudo-spectral methods. These methods expand the solution in terms of a DFS and are an alternative to finite difference and finite element methods. In his original paper [12], Orszag applied a DFS to the solution of the heat equation, to axisymmetric flow, and to the vorticity equation. Yee [16] presented a method for the solution of Poisson's equation on a sphere using a DFS. More recently, Cheong [4,5] developed a spectral transform method incorporating a DFS for the solution of elliptic and vorticity equations, as well as the shallow-water equations. Quite interestingly, most applications of a DFS have their origin in the field of numerical weather prediction.

To the best of our knowledge, Li and Hero [10,11] were the first, and so far the only ones, to apply a DFS to the description of 3D shape. In [11], a fast spectral method for reconstruction of smooth star-shaped 3D surfaces from noisy segmentation data is developed. The authors employ a variational energy minimization approach, where the 3D surface $f(\theta, \phi)$ being sought is specified as a stationary point which minimizes some energy functional. After applying the calculus of variations, an elliptic PDE of

Helmholtz type for $f(\theta, \phi)$ is obtained. That PDE is solved by representing $f(\theta, \phi)$ as a DFS over angles in spherical coordinates.

Some applications require the extraction of spatial-domain features, such as low-order moments and surface area. An important example is content-based 3D model retrieval using moments [13]. Suppose that we have a database of 3D objects stored in the form of their spherical harmonic or DFS coefficients. If the spatial domain features used for matching are known in advance and their number is relatively small, they can be stored for each object in the database. Sometimes, however, each query object has its own set of features that are best suited to find objects that match it. In that case, the spatial-domain features have to be computed online. Extracting features directly from the compact representation eliminates the need for prior object reconstruction and may reduce computational complexity.

In [1], geometric properties of a 3D star-shaped object were expressed directly in terms of the spherical harmonic coefficients of its boundary function. In this work, we calculate the moments of an object from the DFS coefficients. Our results show that the DFS basis is not inferior to spherical harmonics as far as the efficiency of representing 3D objects is concerned, while the complexity of computing the moments from the DFS coefficients is $O(N^2 \log N)$.

Over the years, several kinds of DFS have emerged [2,4,15]. The main difference between the different kinds is the behavior of the basis functions near the poles of a sphere, which affects the accuracy and the speed of convergence of algorithms using a DFS. When a DFS is incorporated in spectral methods for the solution of PDEs, the basis functions are so chosen as to satisfy boundary conditions ensuring that $r(\theta, \phi)$ and its derivatives are continuous at the poles. Let $\{R_m(\theta)\}$, $m \in \mathbb{Z}$, be the complex Fourier coefficients of $r(\theta, \phi)$ expanded as a function of ϕ:

$$R_m(\theta) = \frac{1}{2\pi} \int_{\phi=0}^{2\pi} r(\theta, \phi) e^{-im\phi}\, d\phi \tag{1}$$

$$r(\theta, \phi) = \sum_{m=-\infty}^{\infty} R_m(\theta) e^{im\phi} \tag{2}$$

It is easy to see from (2) that in order for $r(\theta, \phi)$ to be continuous (and therefore single-valued) at the poles, it must hold that

$$R_m(0) = R_m(\pi) = 0 \quad \text{if } m \neq 0 \tag{3}$$

Otherwise, we would have that $r(0, \phi)$ or $r(\pi, \phi)$ depends on the value of ϕ. The condition for the continuity of the derivatives of $r(\theta, \phi)$ is a little more complicated. The key is to observe that for any ϕ, $\frac{\partial r}{\partial \theta}(0, \phi)$ and $-\frac{\partial r}{\partial \theta}(0, \phi + \pi)$ are actually one-sided derivatives along the same latitudinal direction. Consequently, for the latitudinal derivatives of $r(\theta, \phi)$ to be single-valued at $\theta = 0$, it is required that

$$\frac{\partial r}{\partial \theta}(0, \phi) = -\frac{\partial r}{\partial \theta}(0, \phi + \pi) \tag{4}$$

Substituting the Fourier expansion (2) into the last equation, we obtain

$$\sum_{m=-\infty}^{\infty} \frac{dR_m}{d\theta}(0)e^{im\phi} + \sum_{m=-\infty}^{\infty} \frac{dR_m}{d\theta}(0)e^{im(\phi+\pi)} = 0$$

It follows that

$$\frac{dR_m}{d\theta}(0)[1 + (-1)^m] = 0$$

For odd m this condition is satisfied automatically, whereas for even m it implies that $\frac{dR_m}{d\theta}(0) = 0$. The same argument can be applied with regard to the pole at $\theta = \pi$. Therefore, the condition for the continuity of the derivatives of $r(\theta, \phi)$ is that

$$\frac{dR_m}{d\theta}(0) = \frac{dR_m}{d\theta}(\pi) = 0 \quad \text{if } m \text{ is even} \tag{5}$$

Boundary conditions (3) and (5) can be found, for example, in [4]. In order for a solution of a PDE to satisfy (5) automatically, the DFS basis functions are chosen to meet (5). This can be seen by noting that for even m, the DFS basis functions, like spherical harmonics, are even in the latitudinal direction, and an even function, which is 2π-periodic and continuously differentiable, has a zero derivative at $\theta = 0$ and $\theta = \pi$. However, when a DFS is used merely as a means of compact representation, the boundary conditions specific to PDEs can be relaxed. Furthermore, if the boundary function of an object does not satisfy (5), other boundary conditions may be more appropriate. In this work, we exploit this observation and propose a new kind of DFS. We call it the double Fourier sine series, because the functions $R_m(\theta)$, $m \in \mathbb{Z}$, are expanded in a Fourier sine series. We discuss the convergence properties of a DFS and demonstrate that the sine DFS can be advantageous over the previously used kinds and over spherical harmonics for representing an object with a sharp point.

The rest of the paper is organized as follows. In Sect. 2 we recapitulate the definition of a DFS and the relation between a DFS and spherical harmonics. We develop an analogue of the convolution theorem for a DFS in Sect. 3 and use it in Sect. 4 to express the moments of a star-shaped object in terms of the DFS coefficients of its boundary function. In Sect. 5 we propose the double sine Fourier series. In Sect. 6 we show that under sufficient conditions, the moments and surface area corresponding to the truncated DFS converge to the true moments and area of an object. We find that for an object with a sharp point, the sine DFS has better convergence properties than the previously used kinds of DFS as well as than spherical harmonics. We demonstrate it with an example of two synthetic objects. The conclusions are summarized in Sect. 7.

2 DFS on a sphere

Let $\mathbf{r}$ denote the radius vector directed from the origin to a boundary point of a 3D object. Using a spherical coordinate system, $0 \leq \phi < 2\pi$ is the azimuthal angle between the projection of $\mathbf{r}$ onto the xy-plane and the x-axis, $0 \leq \theta \leq \pi$ is the polar angle and r is the distance between the boundary point and the origin. If the function $r(\theta, \phi)$ is single-valued, the object is referred to as *star-shaped*, and $r(\theta, \phi)$ can be represented as a linear combination of some basis functions. The most commonly used basis functions are spherical harmonics [6, §D-1-c of chapter VI and complement $\mathrm{A_{VI}}$], in which case

$$r(\theta, \phi) = \sum_{l=0}^{\infty} \sum_{m=-l}^{l} R_{lm} Y_{lm}(\theta, \phi) \tag{6}$$

where

$$Y_{lm}(\theta, \phi) = \sqrt{\frac{2l+1}{4\pi} \frac{(l-m)!}{(l+m)!}} P_l^m(\cos\theta) e^{im\phi} \quad (m \geq 0) \tag{7}$$

$$Y_{l,-m}(\theta, \phi) = (-1)^m Y_{lm}^*(\theta, \phi) \tag{8}$$

are spherical harmonics, $P_l^m(\cos\theta)$ are associated Legendre functions, and * denotes complex conjugation. The coefficients $\{R_{lm}\}$ of a spherical harmonic series form a spatial frequency domain representation of an object. The shape can be usually well approximated with a small set of coefficients. The main reason for the wide use of spherical harmonics is probably that they arise naturally as eigenfunctions of the Laplace equation on a sphere.

As we have mentioned, the relatively high computational complexity of the SHT is caused by the associated Legendre functions $P_l^{|m|}(\cos\theta)$. Obviously, we would like to work with a representation of functions on a sphere for which the transformation between the spatial and the frequency domains can be done in $O(N^2 \log N)$ operations, where N is the maximum order of frequency-domain coefficients, similarly to a Fourier series in the Cartesian coordinates. Orszag [12] devised such a representation by noting that the associated Legendre functions can be written as [6, p. 687]

$$P_l^{|m|}(\cos\theta) = (\sin\theta)^{|m|} q_l^{|m|}(\cos\theta) \tag{9}$$

where $q_l^{|m|}(x)$ is a polynomial in x of degree $l - |m|$. For any $0 \leq s \leq |m|$ we have

$$(\sin\theta)^{|m|} = \sin^s\theta(1 - \cos^2\theta)^{(|m|-s)/2} \tag{10}$$

Let us choose

$$s = \begin{cases} 0 & \text{if } m \text{ is even} \\ 1 & \text{if } m \text{ is odd} \end{cases} \tag{11}$$

Substituting (10) into (9), we obtain

$$P_l^{|m|}(\cos\theta) = \sin^s\theta \, {q'}_l^{|m|}(\cos\theta)$$

where ${q'}_l^{|m|}(x) = (1-x^2)^{(|m|-s)/2} q_l^{|m|}(x)$ is a polynomial in x of degree $l-s$. At this point we employ the fact that $\cos^k\theta$ can be represented as a linear combination of $\cos(n\theta)$, $n = 0, \dots, k$. Hence there exist coefficients $A_{l,|m|,n}$ such that

$$P_l^{|m|}(\cos\theta) = \sin^s\theta \sum_{n=0}^{l-s} A_{l,|m|,n}\cos(n\theta) \tag{12}$$

Now consider a function $r(\theta, \phi)$ which is expandable into a series of spherical harmonics up to order N:

$$r(\theta,\phi) = \sum_{l=0}^{N}\sum_{m=-l}^{l} Q_{lm} P_l^{|m|}(\cos\theta) e^{im\phi} = \sum_{m=-N}^{N}\left[\sum_{l=|m|}^{N} Q_{lm} P_l^{|m|}(\cos\theta)\right] e^{im\phi} \tag{13}$$

From (12) we see that for all m the expression in square brackets in (13) is $\sin^s\theta$ times a linear combination of $\cos(n\theta)$, $n = 0, \dots, N$. Therefore, $r(\theta, \phi)$ can be also written as

$$r(\theta,\phi) = \sum_{m=-N}^{N} \sin^s\theta \left[\sum_{n=0}^{N} \rho_{nm}\cos(n\theta)\right] e^{im\phi} \tag{14}$$

where ρ_{nm} are some coefficients. We have that $r(\theta, \phi)$ can be expanded in the following series:

$$r(\theta,\phi) = \sum_{n=0}^{N}\sum_{m=-N}^{N} \rho_{nm} \sin^s\theta \cos(n\theta) e^{im\phi} \tag{15}$$

We define the Fourier functions as

$$Z_{nm}(\theta,\phi) = \sin^s\theta\cos(n\theta)e^{im\phi} \tag{16}$$

Expansions of the form (15) are called Fourier series on spheres, or DFS. We have shown that any function $r(\theta, \phi)$ in the subspace spanned by spherical harmonics up to order N can be also expanded in a DFS up to order N. Note that the opposite is not necessarily true, since the number of the Fourier functions in Eq. (15) is $(N+1)(2N+1)$, whereas the number of the spherical harmonics in Eq. (13) is only $(N+1)^2$. It follows that the Fourier functions $Z_{nm}(\theta, \phi)$, like spherical harmonics, form a complete basis for functions defined on the surface of a sphere. The DFS coefficients ρ_{nm} in (15) are calculated as [15]

$$\rho_{nm} = \frac{c}{\pi}\int_{\theta=0}^{\pi} \frac{1}{\sin^s\theta} R_m(\theta)\cos(n\theta)\,d\theta \tag{17}$$

with $c = 1$ for $n = 0$, $c = 2$ for $n \neq 0$, and $R_m(\theta)$ given by (1).

Another kind of DFS, due to Yee [15], uses Fourier cosine series for even m and sine series for odd m:

$$r(\theta, \phi) = \sum_{n=0}^{\infty} \sum_{m=-\infty}^{\infty} \lambda_{nm} \left[(1-s)\cos(n\theta) + s\sin(n\theta)\right] e^{im\phi} \tag{18}$$

The expansion coefficients λ_{nm} are given by

$$\lambda_{nm} = \frac{c}{\pi} \int_{\theta=0}^{\pi} R_m(\theta) \left[(1-s)\cos(n\theta) + s\sin(n\theta)\right] d\theta \tag{19}$$

where s, c, and $R_m(\theta)$ are the same as previously defined.

In this work, we use expansions (15) and (18). Note that throughout this paper, we use s to denote the exponent of $\sin\theta$ in the Fourier basis functions (16). It is determined from the corresponding index m according to (11).

3 The Fourier coefficients of a product of functions

Next we develop an analogue of the convolution theorem for the DFS of Eq. (15). Given the Fourier coefficients of two functions $f(\theta, \phi)$ and $g(\theta, \phi)$, our goal is to compute the coefficients of $h(\theta, \phi) = f(\theta, \phi)g(\theta, \phi)$. For purely technical reasons that will become evident in the sequel, it will be more convenient for us to work with complex exponentials in θ rather than cosines. To this end, we rewrite (15) as

$$r(\theta, \phi) = \sum_{n=-\infty}^{\infty} \sum_{m=-\infty}^{\infty} F_{nm} \sin^s \theta e^{in\theta} e^{im\phi} \tag{20}$$

We see that the coefficients of this expansion are related to those of (15) by

$$F_{nm} = \begin{cases} \rho_{0,m} & \text{if } n = 0 \\ \frac{1}{2}\rho_{|n|,m} & \text{if } n \neq 0 \end{cases} \tag{21}$$

We call F_{nm} the spherical Fourier coefficients to distinguish them from the usual Cartesian Fourier coefficients. Now assume that F_{nm} and G_{nm} are the respective spherical Fourier coefficients of $f(\theta, \phi)$ and $g(\theta, \phi)$. Let us decompose F_{nm} into even and odd components, namely

$$F_{nm}^{\text{even}} = \begin{cases} F_{nm} & \text{if } m \text{ is even} \\ 0 & \text{if } m \text{ is odd} \end{cases} \tag{22}$$

and

$$F_{nm}^{\text{odd}} = \begin{cases} 0 & \text{if } m \text{ is even} \\ F_{nm} & \text{if } m \text{ is odd} \end{cases} \tag{23}$$

We define $f^{\text{even}}(\theta, \phi)$ and $f^{\text{odd}}(\theta, \phi)$ as the functions whose spherical Fourier coefficients are equal to F_{nm}^{even} and F_{nm}^{odd}, respectively:

$$f^{\text{even}}(\theta, \phi) = \sum_{n=-\infty}^{\infty} \sum_{m=-\infty}^{\infty} F_{nm}^{\text{even}} \sin^s \theta e^{in\theta} e^{im\phi} \tag{24}$$

$$f^{\text{odd}}(\theta, \phi) = \sum_{n=-\infty}^{\infty} \sum_{m=-\infty}^{\infty} F_{nm}^{\text{odd}} \sin^s \theta e^{in\theta} e^{im\phi} \tag{25}$$

Alternatively, F_{nm}^{even} and F_{nm}^{odd} can be viewed as the Cartesian Fourier coefficients of some functions $\widetilde{f}^{\text{even}}$ and $\widetilde{f}^{\text{odd}}$:

$$\widetilde{f}^{\text{even}}(\theta, \phi) = \sum_{n=-\infty}^{\infty} \sum_{m=-\infty}^{\infty} F_{nm}^{\text{even}} e^{in\theta} e^{im\phi} \tag{26}$$

$$\widetilde{f}^{\text{odd}}(\theta, \phi) = \sum_{n=-\infty}^{\infty} \sum_{m=-\infty}^{\infty} F_{nm}^{\text{odd}} e^{in\theta} e^{im\phi} \tag{27}$$

Since, by (11), s is 0 for even m and 1 for odd m, we have

$$f^{\text{even}}(\theta, \phi) = \widetilde{f}^{\text{even}}(\theta, \phi) \tag{28}$$

$$f^{\text{odd}}(\theta, \phi) = \sin \theta \widetilde{f}^{\text{odd}}(\theta, \phi) \tag{29}$$

The decomposition into even and odd components is also applied to G_{mn}, and G_{nm}^{even}, G_{nm}^{odd}, $g^{\text{even}}(\theta, \phi)$, $g^{\text{odd}}(\theta, \phi)$, $\widetilde{g}^{\text{even}}(\theta, \phi)$ and $\widetilde{g}^{\text{odd}}(\theta, \phi)$ are defined similarly to their F-counterparts. Now, using (28) and (29), we can write $h(\theta, \phi)$ in the form

$$\begin{aligned} h(\theta, \phi) &= [f^{\text{even}}(\theta, \phi) + f^{\text{odd}}(\theta, \phi)][g^{\text{even}}(\theta, \phi) + g^{\text{odd}}(\theta, \phi)] \\ &= h^{(1)}(\theta, \phi) + \sin \theta h^{(2)}(\theta, \phi) + \sin \theta h^{(3)}(\theta, \phi) + \sin^2 \theta h^{(4)}(\theta, \phi) \end{aligned} \tag{30}$$

where we defined:

$$h^{(1)}(\theta, \phi) = \widetilde{f}^{\text{even}}(\theta, \phi) \widetilde{g}^{\text{even}}(\theta, \phi) \tag{31}$$

$$h^{(2)}(\theta, \phi) = \widetilde{f}^{\text{even}}(\theta, \phi) \widetilde{g}^{\text{odd}}(\theta, \phi) \tag{32}$$

$$h^{(3)}(\theta, \phi) = \widetilde{f}^{\text{odd}}(\theta, \phi) \widetilde{g}^{\text{even}}(\theta, \phi) \tag{33}$$

$$h^{(4)}(\theta, \phi) = \widetilde{f}^{\text{odd}}(\theta, \phi) \widetilde{g}^{\text{odd}}(\theta, \phi) \tag{34}$$

According to the convolution theorem well-known from the 2D Fourier theory, multiplication in the spatial domain is equivalent to convolution in the coefficients domain.

Therefore, the functions $h^{(k)}(\theta, \phi)$, $k = 1, \ldots, 4$, can be expanded in the Cartesian Fourier series as

$$h^{(k)}(\theta, \phi) = \sum_{n=-\infty}^{\infty} \sum_{m=-\infty}^{\infty} H_{nm}^{(k)} e^{in\theta} e^{im\phi} \tag{35}$$

where the coefficients $H_{nm}^{(k)}$ are computed by convolution of the even and the odd components of F_{nm} and G_{nm}:

$$H_{nm}^{(1)} = F_{nm}^{\text{even}} * G_{nm}^{\text{even}} = \sum_{n'=-\infty}^{\infty} \sum_{m'=-\infty}^{\infty} F_{n'm'}^{\text{even}} G_{n-n',m-m'}^{\text{even}} \tag{36}$$

$$H_{nm}^{(2)} = F_{nm}^{\text{even}} * G_{nm}^{\text{odd}} \tag{37}$$

$$H_{nm}^{(3)} = F_{nm}^{\text{odd}} * G_{nm}^{\text{even}} \tag{38}$$

$$H_{nm}^{(4)} = F_{nm}^{\text{odd}} * G_{nm}^{\text{odd}} \tag{39}$$

Let us consider $h^{(1)}$ first. From (36) it follows that since both F_{nm}^{even} and G_{nm}^{even} are zero for odd m, so is $H_{nm}^{(1)}$. Using the fact that s, the exponent of $\sin\theta$ in the Fourier basis functions, is zero for even m [by Eq. (11)], we get from (35):

$$h^{(1)}(\theta, \phi) = \sum_{n=-\infty}^{\infty} \sum_{m=-\infty}^{\infty} H_{nm}^{(1)} \sin^s \theta e^{in\theta} e^{im\phi} \tag{40}$$

The last equation says that $H_{nm}^{(1)}$ are the spherical Fourier coefficients of $h^{(1)}(\theta, \phi)$. Next we look at $h^{(2)}(\theta, \phi)$. F_{nm}^{even} are different from zero only for even m, and G_{nm}^{odd} are different from zero only for odd m. Therefore, from (37) we conclude that $H_{nm}^{(2)}$ are different from zero only for odd m. Multiplying both sides of (35) by $\sin\theta$ and bearing in mind that, according to (11), $s = 1$ for odd m, we obtain that $H_{nm}^{(2)}$ are the spherical Fourier coefficients of $\sin\theta h^{(2)}(\theta, \phi)$:

$$\sin\theta h^{(2)}(\theta, \phi) = \sum_{n=-\infty}^{\infty} \sum_{m=-\infty}^{\infty} H_{nm}^{(2)} \sin^s \theta e^{in\theta} e^{im\phi} \tag{41}$$

In a similar way, it can be shown that $H_{nm}^{(3)}$ are the spherical Fourier coefficients of $\sin\theta h^{(3)}(\theta, \phi)$. Finally, let us consider the fourth term on the right-hand side of (30). Using the relationship $\sin^2\theta = -\frac{1}{4}(e^{2i\theta} + e^{-2i\theta} - 2)$, (35) gives

$$\sin^2\theta h^{(2)}(\theta, \phi) = -\frac{1}{4} \sum_{n=-\infty}^{\infty} \sum_{m=-\infty}^{\infty} \left[H_{n-2,m}^{(4)} + H_{n+2,m}^{(4)} - 2H_{nm}^{(4)} \right] e^{in\theta} e^{im\phi} \tag{42}$$

Since F_{nm}^{odd} and G_{nm}^{odd} are different from zero only for odd m, from (39) we see that $H_{nm}^{(4)}$ are different from zero only for even m. It follows that the spherical Fourier coefficients of $\sin^2\theta h^{(4)}(\theta,\phi)$ are equal to $-\frac{1}{4}[H^{(4)}_{n-2,m}+H^{(4)}_{n+2,m}-2H^{(4)}_{nm}]$. Now, by combining (30) and (36–42) we get the following expression for the spherical Fourier coefficients of the product $f(\theta,\phi)g(\theta,\phi)$:

$$H_{nm}=F^{\text{even}}_{nm}*G^{\text{even}}_{nm}+F^{\text{even}}_{nm}*G^{\text{odd}}_{nm}+F^{\text{odd}}_{nm}*G^{\text{even}}_{nm}-\frac{1}{4}\left[H^{(4)}_{n-2,m}+H^{(4)}_{n+2,m}-2H^{(4)}_{nm}\right]$$

Adding and subtracting $H^{(4)}_{n,m}$ to the right-hand side, we arrive at the final form for H_{nm}:

$$H_{nm}=F_{nm}*G_{nm}-\frac{1}{4}\left[2H^{(4)}_{nm}+H^{(4)}_{n-2,m}+H^{(4)}_{n+2,m}\right] \tag{43}$$

We see from this equation that to obtain the spherical Fourier coefficients of a product of two functions, we need to perform two convolutions, the first between $\{F_{nm}\}$ and $\{G_{nm}\}$ and the second between $\{F^{\text{odd}}_{nm}\}$ and $\{G^{\text{odd}}_{nm}\}$. The convolutions can be implemented via the 2D FFT. Hence, assuming that $F_{nm}=0$ and $G_{nm}=0$ for $|n|>N$ or $|m|>N$, the complexity of computing $\{H_{nm}\}$ is $O(N^2\log N)$.

4 Calculating the moments of a 3D object from the DFS representation

In this section we discuss how to express the moments of a star-shaped object in terms of the spherical Fourier coefficients $\{R_{nm}\}$ of its boundary function $r(\theta,\phi)$. The moments of the object are given by

$$\begin{aligned}
M_{ijk} &= \int\limits_{Object} x^i y^j z^k\,dv\\
&= \int\limits_{\theta=0}^{\pi}\int\limits_{\phi=0}^{2\pi}\int\limits_{\rho=0}^{r(\theta,\phi)} (\rho\sin\theta\cos\phi)^i(\rho\sin\theta\sin\phi)^j(\rho\cos\theta)^k\rho^2\sin\theta\,d\rho\,d\phi\,d\theta\\
&= \frac{1}{i+j+k+3}\int\limits_{\theta=0}^{\pi}\int\limits_{\phi=0}^{2\pi} r^{i+j+k+3}(\theta,\phi)\\
&\quad\times(\sin\theta)^{i+j+1}\cos^i\phi\sin^j\phi\cos^k\theta\,d\phi\,d\theta
\end{aligned} \tag{44}$$

For each $l=1,2,\ldots,$ let $\{P^l_{nm}\}$ denote the spherical Fourier coefficients of $r^l(\theta,\phi)$. The last equation then reads

$$\begin{aligned}
M_{ijk} &= \frac{1}{i+j+k+3}\int\limits_{\theta=0}^{\pi}\int\limits_{\phi=0}^{2\pi}\left[\sum_{n=-\infty}^{\infty}\sum_{m=-\infty}^{\infty}P^{i+j+k+3}_{nm}\sin^s\theta e^{in\theta}e^{im\phi}\right]\\
&\quad\times(\sin\theta)^{i+j+1}\cos^i\phi\sin^j\phi\cos^k\theta\,d\phi\,d\theta
\end{aligned} \tag{45}$$

Fig. 1 Mannequin head

We define

$$I_{nm}^{ijk} = \frac{1}{i+j+k+3} \int_{\theta=0}^{\pi} \int_{\phi=0}^{2\pi} e^{in\theta} e^{im\phi} (\sin\theta)^{i+j+1+s} \cos^i\phi \sin^j\phi \cos^k\theta \, d\phi \, d\theta \tag{46}$$

The integrals in the expressions I_{nm}^{ijk} are independent of $r(\theta, \phi)$, so they can be calculated offline numerically. It follows then from (45) that the moment M_{ijk} can be expressed as

$$M_{ijk} = \sum_{n=-\infty}^{\infty} \sum_{m=-\infty}^{\infty} P_{nm}^{i+j+k+3} I_{nm}^{ijk} \tag{47}$$

We have thus shown that in order to obtain the moments of an object, it is sufficient to know $\{P_{nm}^{i+j+k+3}\}$. According to Sect. 3, $\{P_{nm}^{i+j+k+3}\}$ can be calculated from $\{R_{nm}\}$ by repetitive application of (43). The complexity of computing the moments from the DFS coefficients is therefore $O(N^2 \log N)$.

To verify the proposed method, we calculated the volume, location of the centroid, and second-order moments of the mannequin head shown in Fig. 1 via the DFS coefficients. We compared the results with those of [1], where the moments of the same mannequin head were calculated from its spherical harmonic representation as well as directly in the spatial domain. Both the spherical harmonic series and the DFS were truncated at the order $N = 8$. The comparison results are summarized in Table 1. As we can see, for the same maximum order of coefficients retained in the expansion, the DFS and the spherical harmonic methods achieve very similar accuracy. This is in agreement with the fact that any function $r(\theta, \phi)$ that is expandable into a series of spherical harmonics up to order N can be also represented as a linear combination of the Fourier functions up to order N. Also note that the number of coefficients to

Table 1 Moments of the mannequin head computed from the DFS coefficients, in reference to the directly computed values and to the spherical harmonic method

Moment type	DFS for $N = 8$	Direct calculation	Error (%)	Error of the spherical harmonic method for $l = 8$ (%)[a]
V	3.5915	3.5977	0.17	0.17
M_x	−0.0957	−0.0945	1.27	1.35
M_y	−0.0931	−0.0930	0.11	0.08
M_z	0.1172	0.1174	0.17	0.08
M_{xx}	0.9611	0.9675	0.66	0.83
M_{xy}	0.0927	0.0930	0.32	0.58
M_{xz}	−0.2000	−0.2007	0.35	0.23
M_{yy}	0.5054	0.5073	0.37	0.45
M_{yz}	−0.0554	−0.0557	0.54	0.53
M_{zz}	0.7547	0.7575	0.37	0.24

[a] The values calculated from the spherical harmonic representation are taken from [1]

be stored is $O(N^2)$ in both methods. We thus conclude that the DFS expansion is advantageous, as it has lower computational complexity.

5 Double Fourier sine series

In this section we propose an alternative DFS expansion that we call the double Fourier sine series. Consider a function $r(\theta, \phi)$ defined on a sphere. For each $0 \leq \theta \leq \pi$, $r(\theta, \phi)$ can be viewed as a function of the single variable ϕ. We expand $r(\theta, \phi)$ in a complex Fourier series in ϕ. The corresponding Fourier coefficients $R_m(\theta)$, $m \in \mathbb{Z}$, are given by (1).

Let us now examine the functions $R_m(\theta)$. As we saw in Sect. 1, for $r(\theta, \phi)$ to be single-valued at the poles, they must satisfy condition (3), i.e. $R_m(0) = R_m(\pi) = 0$ for every $m \neq 0$. Therefore, for $m \neq 0$ $R_m(\theta)$ can be naturally expanded in a Fourier sine series. This means that we make an odd extension of $R_m(\theta)$ to $[-\pi, 0]$. The derivative of the extended function is then continuous at $\theta = 0$ and $\theta = \pi$.

Contrary to other values of m, $R_0(\theta)$ is different from zero at $\theta = 0$ and $\theta = \pi$. One possibility is to expand it in a Fourier cosine series. This is equivalent to making an even extension of $R_0(\theta)$ to $[-\pi, 0]$. But since $\frac{dR}{d\theta}(0)$ and $\frac{dR}{d\theta}(\pi)$ are in general different from zero, the derivative of the extended function will not be continuous at $\theta = 0$ and $\theta = \pi$. To achieve continuity of the derivative, we subtract from $R_0(\theta)$ a straight line that passes through $R_0(0)$ and $R_0(\theta)$ and define

$$\tilde{R}_m(\theta) = \begin{cases} R_0(\theta) - A - B\theta & \text{if } m = 0 \\ R_m(\theta) & \text{otherwise} \end{cases} \tag{48}$$

where

$$A = R_0(0) \tag{49}$$

$$B = \frac{R_0(\pi) - R_0(0)}{\pi} \tag{50}$$

Defined in this way, the functions $\tilde{R}_m(\theta)$ vanish at $\theta = 0$ and $\theta = \pi$ for all m, so their odd extension to $[-\pi, 0]$ will have a continuous first derivative at $\theta = 0$ and $\theta = \pi$. We expand $\tilde{R}_m(\theta)$ in a Fourier sine series with the coefficients of the series given by

$$\rho_{nm} = \frac{2}{\pi} \int_0^{\pi} \tilde{R}_m(\theta) \sin(n\theta)\, d\theta \quad n = 1, 2, \ldots \tag{51}$$

This gives the following expression for the double Fourier sine series:

$$r(\theta, \phi) = A\theta + B + \sum_{m=-\infty}^{\infty} \sum_{n=1}^{\infty} \rho_{nm} \sin(n\theta) e^{im\phi} \tag{52}$$

We have thus shown that the sine DFS can be obtained by a reasoning very similar to the one used for a two-dimensional Fourier series in the Cartesian plane, without the need to go through the spherical harmonic expansion.

6 Convergence of geometric properties

As in the case of spherical harmonics, there is a question as to under which conditions the moments and surface area corresponding to partial sums of a DFS converge to the true moments and area. We first formulate and prove conditions for convergence in the case of the sine DFS and then discuss the differences between the sine DFS and the standard kinds of DFS given by (15) and (18). Let us denote by $r_{NM}(\theta, \phi)$ a partial sum of the sine DFS of Eq. (52):

$$r_{NM}(\theta, \phi) = A\theta + B + \sum_{m=-M}^{M} \sum_{n=1}^{N} \rho_{nm} \sin(n\theta) e^{im\phi} \tag{53}$$

We claim the following:

1. Assume that $r(\theta, \phi)$ is continuous, and the partial derivatives $\partial r/\partial\theta$ and $\partial r/\partial\phi$ are piecewise continuous. If in addition $r(\theta, \phi)$ is well-behaved in a sense that we will define in the sequel, then there exists a path in the NM-plane along which the sequence of moments corresponding to $r_{NM}(\theta, \phi)$ converges to the true moment of the object described by $r(\theta, \phi)$.

2. If the partial derivatives $\partial r/\partial\theta$ and $\partial r/\partial\phi$ are continuous and well-behaved in the same sense as in claim 1, and the second derivatives of r are piecewise continuous, then there exists a path in the NM-plane along which the sequence of surface areas corresponding to $r_{NM}(\theta,\phi)$ converges to the true surface area.

We start by showing that if the conditions of claim 1 are satisfied, there is a path in the NM-plane along which the sine DFS $r_{NM}(\theta,\phi)$ converges uniformly on the sphere to $r(\theta,\phi)$. Our argument is based on the uniform convergence theorem for a one-dimensional Fourier series [14, p. 84], which says that if function $f(x)$ is continuous for $-\pi \le x \le \pi$, $f(-\pi) = f(\pi)$, and the derivative df/dx is piecewise continuous, then the Fourier series of $f(x)$ converges to $f(x)$ uniformly.

As previously, for each $0 \le \theta \le \pi$ we can expand $r(\theta,\phi)$ in a complex Fourier series in ϕ with the coefficients $R_m(\theta)$ given by (1). Since $r(\theta,\phi)$ is continuous, $r(\theta,0) = r(\theta,2\pi)$, and $\partial r/\partial\phi$ is piecewise continuous, it follows that the Fourier series in ϕ converges uniformly in $[0,2\pi]$ to $r(\theta,\phi)$. Therefore, for any $\varepsilon > 0$ there exists $0 < M_1(\theta) < \infty$ such that for every $M \ge M_1(\theta)$ and every $\phi \in [0,2\pi]$

$$\left|\sum_{m=-M}^{M} R_m(\theta)e^{im\phi} - r(\theta,\phi)\right| < \frac{\varepsilon}{2} \tag{54}$$

We consider $r(\theta,\phi)$ to be well-behaved if $M_1(\theta)$ is upper-bounded, i.e. there exists $M_0 < \infty$ such that Eq. (54) holds for every $M \ge M_0$ and for every $(\theta,\phi) \in [0,\pi] \times [0,2\pi]$.

The functions $\tilde{R}_m(\theta)$ defined in Eq. (48) are continuous at every point in $(0,\pi)$, because $R_m(\theta)$ is an integral of the continuous function $r(\theta,\phi)e^{-im\phi}$. Since $\tilde{R}_m(0) = \tilde{R}_m(\pi) = 0$, if we make an odd extension of $\tilde{R}_m(\theta)$ to $[-\pi,0]$, the extended function is continuous at $\theta = 0$ and $\theta = \pi$. The derivatives $d\tilde{R}_m/d\theta$ are piecewise continuous, as $dR_m/d\theta$ is an integral of the piecewise continuous function $\frac{\partial r}{\partial\theta}e^{-im\phi}$. According to the uniform convergence theorem for a one-dimensional Fourier series, it follows that for each m the sine DFS of $\tilde{R}_m(\theta)$ converges uniformly in $[0,\pi]$ to $\tilde{R}_m(\theta)$. Therefore, given $\varepsilon > 0$ and $M \ge M_0$ as defined previously, for each $-M \le m \le M$ there exists $N_1(m)$ such that for every $N \ge N_1(m)$ and every $\theta \in [0,\pi]$

$$\left|\sum_{n=1}^{N} \rho_{nm}\sin(n\theta) - \tilde{R}_m(\theta)\right| < \frac{\varepsilon}{2(2M+1)} \tag{55}$$

Let us define

$$N_0(M) = \max_{-M\le m\le M} N_1(m)$$

Then Eq. (55) holds for every $N \ge N_0(m)$. Combining (54) and (55), we can write:

$$
\begin{aligned}
&\left|A\theta + B + \sum_{m=-M}^{M}\sum_{n=1}^{N} \rho_{nm}\sin(n\theta)e^{im\phi} - r(\theta,\phi)\right| \\
&\quad = \left|A\theta + B + \sum_{n=1}^{N}\rho_{n0}\sin(n\theta) + \sum_{|m|=1}^{M}\sum_{n=1}^{N}\rho_{nm}\sin(n\theta)e^{im\phi}\right. \\
&\qquad \left. - \sum_{m=-M}^{M} R_m(\theta)e^{im\phi} + \sum_{m=-M}^{M} R_m(\theta)e^{im\phi} - r(\theta,\phi)\right| \\
&\quad \le \left|\left\{\sum_{n=1}^{N}\rho_{n0}\sin(n\theta) - [R_0(\theta) - A - B\theta]\right\} e^{im\phi}\right| \\
&\qquad + \sum_{|m|=1}^{M}\left|\left[\sum_{n=1}^{N}\rho_{nm}\sin(n\theta) - R_m(\theta)\right] e^{im\phi}\right| + \left|\sum_{m=-M}^{M} R_m e^{im\phi} - r(\theta,\phi)\right| \\
&\quad \le \frac{\varepsilon}{2(2M+1)} + 2M\frac{\varepsilon}{2(2M+1)} + \frac{\varepsilon}{2} = \varepsilon
\end{aligned}
$$

We have thus obtained that for for any $\varepsilon > 0$ there exists M_0 such that for every $M \ge M_0$ there exists $N_0(M)$ such that for any $N \ge N_0(M)$ and for any $(\theta,\phi) \in [0,\pi] \times [0,2\pi]$, the absolute difference between $r(\theta,\phi)$ and the partial sum of its sine DFS $r_{NM}(\theta,\phi)$ is smaller than ε. It means that along the path $N = N_0(M)$, $r_{NM}(\theta,\phi)$ converges uniformly on the sphere to $r(\theta,\phi)$. It is proved in [1] that the uniform convergence of a truncated series of the boundary function is a sufficient condition for the convergence of the moments corresponding to the truncated series to the true moments.

Let us turn now to the surface area. As is shown in [1], a sufficient condition for the convergence of the surface areas is that the truncated series of $\partial r/\partial\theta$ and $\partial r/\partial\phi$ converge uniformly on the sphere. Applying the same argument as we have used for $r(\theta,\phi)$, we can show that if the conditions of claim 2 are satisfied, there is a path in the NM-plane along which the sine DFS of $\partial r/\partial\phi$ converges uniformly on the sphere to $\partial r/\partial\phi$. Regarding $\partial r/\partial\theta$, recall from Sect. 5 that the functions $\tilde{R}_m(\theta)$ are zero at $\theta = 0$ and $\theta = \pi$, so their odd extension to $[-\pi, 0]$ has a continuous first derivative. Consequently, the sine DFS of $\tilde{R}_m(\theta)$ converges uniformly in $[0,\pi]$ to $\tilde{R}_m(\theta)$. Having noted that, we can apply the above argument once again to show that there is a path in the NM-plane along which the sine DFS of $\partial r/\partial\theta$ converges uniformly on the sphere to $\partial r/\partial\theta$. This concludes the proof of the convergence of geometric properties.

It is now evident from the above discussion in what cases the sine DFS can be advantageous over other kinds of DFS as well as over spherical harmonics. As we mentioned in Sect. 1, for even values of m the basis functions of other kinds of DFS and the spherical harmonics are even in the latitudinal direction. When we expand $R_m(\theta)$ in a basis of even functions, we essentially make an even extension of $R_m(\theta)$ to $[-\pi, 0]$. If the derivative $dR_m/d\theta$ is different from zero at $\theta = 0$ or $\theta = \pi$, the extended function will not have a continuous first derivative. Consequently, unless for all even m the derivatives $dR_m/d\theta$ are zero at both $\theta = 0$ and $\theta = \pi$, the expansion of $\partial r/\partial\theta$ does not in general converge uniformly. In this case, the convergence of the moments is still guaranteed, but the sequence of surface areas may not converge to the true area, or at least the convergence is much slower than for the sine DFS. Note that the above condition for the convergence of the surface area is exactly the same as (5), which is the condition for the continuity of the latitudinal derivative of $r(\theta, \phi)$ at the poles. Therefore, for other kinds of DFS and for the spherical harmonic representation, the surface area is guaranteed to converge to the true value only if the first derivatives of $r(\theta, \phi)$ are continuous at the poles. From the geometrical point of view, the discontinuity of the derivatives of $r(\theta, \phi)$ at $\theta = 0$ or $\theta = \pi$ indicates that the object has a sharp point above the pole of the spherical domain. It follows that the sine DFS can be beneficial for representing an object with a sharp point, because we can choose the coordinate system in such a way that the sharp point is above one of the poles.

To demonstrate the advantage of the sine DFS quantitatively, we considered two synthetic objects. The first is given by

$$r_1(\theta, \phi) = \sqrt{[r_{a1}(\theta)\cos\theta]^2 + [r_{a1}(\theta) r_b(\phi)\sin\theta]^2} \tag{56}$$

where

$$r_{a1}(\theta) = \begin{cases} 1 & \text{if } 0 \le \theta < \pi/2 \\ \left(\frac{2\theta}{\pi} - 1\right)^2 + 1 & \text{if } \pi/2 \le \theta < 3\pi/4 \\ \frac{3}{2} - \left(2 - \frac{2\theta}{\pi}\right)^2 & \text{if } 3\pi/4 \le \theta \le \pi \end{cases} \tag{57}$$

and

$$r_b(\phi) = \frac{1}{2}(\cos\phi + \sqrt{\cos^2\phi + 3}) \tag{58}$$

The second object is given by

$$r_2(\theta, \phi) = \sqrt{[r_{a2}(\theta)\cos\theta]^2 + [r_{a2}(\theta) r_b(\phi)\sin\theta]^2} \tag{59}$$

where

$$r_{a2}(\theta) = \begin{cases} 1 & \text{if } 0 \le \theta < \pi/2 \\ \left(\frac{2\theta}{\pi} - 1\right)^2 + 1 & \text{if } \pi/2 \le \theta \le \pi \end{cases} \tag{60}$$

and $r_b(\phi)$ is as in (58). As can be seen, for the first object the derivatives $dR_m/d\theta$ are zero at $\theta = 0$ and $\theta = \pi$, whereas for the second object they are different from zero at $\theta = \pi$. Consequently, the first object is smooth everywhere, while the second object has a sharp point above the pole $\theta = \pi$. We calculated the surface areas of the two objects from Yee's DFS of Eq. (18), the sine DFS, and the spherical harmonic series and compared them with the true surface areas computed directly in the spatial domain. The results of calculations by the three methods are summarized in Tables 2, 3, and

Table 2 Surface area of synthetic object no. 1 computed from Yee's DFS of Eq. (18), the sine DFS, and the spherical harmonic series

N	Yee's DFS of Eq. (18) truncated at order N	Sine DFS truncated at order N	Spherical harmonic series truncated at order N
1	17.1458	15.797	15.727
2	16.2112	15.8941	16.2646
3	16.3667	16.369	16.4098
4	16.4011	16.4323	16.4175
5	16.4201	16.4255	16.4237
6	16.4285	16.4287	16.4252
7	16.4319	16.4317	16.4299
8	16.4321	16.4317	16.4301

The true value of the surface area is 16.4318. For the smooth object, the values of the surface area converge rapidly and at about the same rate for all three expansions

Table 3 Surface area of synthetic object no. 2 computed from Yee's DFS of Eq. (18), the sine DFS, and the spherical harmonic series

N	Yee's DFS of Eq. (18) truncated at order N	Sine DFS truncated at order N	Spherical harmonic series truncated at order N
1	18.657	17.6035	16.1796
2	17.4581	17.1989	16.9481
3	17.6594	17.3847	17.2221
4	17.4993	17.3875	17.2664
5	17.448	17.3765	17.2871
6	17.4287	17.3738	17.3116
7	17.424	17.3728	17.3309
8	17.4082	17.3725	17.3381
9	17.3984	17.3711	17.3423
10	17.3941	17.3707	17.3474
11	17.3921	17.3703	17.352
12	17.388	17.3703	17.3545

The true value of the surface area is 17.3695. For the object with a sharp point above the pole, the values of the surface area calculated from the sine DFS converge much faster compared to the other two expansions

Fig. 2 presents the error in the surface area as a function of the maximum order N of the coefficients retained in the expansion. We can see that in the case of the first object, the values of the surface area converge rapidly and at about the same rate for all three expansions. For the second object, the values calculated from the sine DFS converge similarly fast. The surface areas calculated from Yee's DFS of Eq. (18) and from the spherical harmonic series, however, approach the true value at a much slower rate. These results are therefore in agreement with our theoretical analysis.

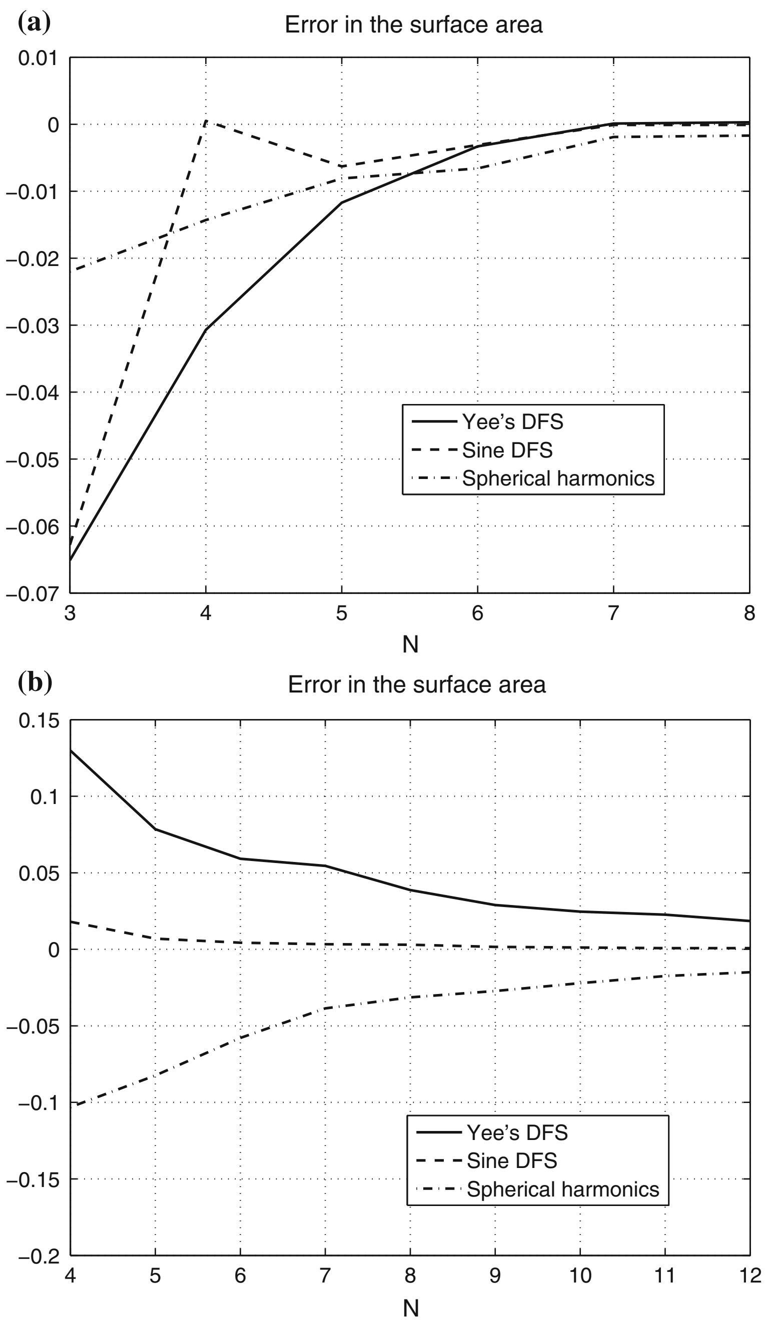

Fig. 2 Error in the surface area calculated by the three methods as a function of the maximum order N of the coefficients retained in the expansion: **a** synthetic object no. 1; **b** synthetic object no. 2

7 Conclusions

In this work, the representation of 3D star-shaped objects by the DFS coefficients of their boundary function has been studied. We expressed the moments of an object directly in terms of the DFS coefficients, without an intermediate reconstruction step, and showed that this method has lower computational complexity compared to the spherical harmonic one for the same accuracy. This result suggests that while spherical harmonics are the most common basis for frequency representation of 3D objects, a DFS can be actually preferable for some applications. In addition, we proposed a new kind of DFS—the double Fourier sine series—and demonstrated that it can be advantageous over the previously used kinds and over spherical harmonics for representing an object with a sharp point.

References

1. Baxansky A, Kiryati N (2007) Calculating geometric properties of three-dimensional objects from the spherical harmonic representation. Pattern Recognit 40:756–770
2. Boer GJ, Steinberg L (1975) Fourier series on spheres. Atmosphere 13:180–191
3. Brechbühler Ch, Gerig G, Kübler O (1995) Parameterization of closed surfaces for 3-D shape description. Comput Vis Image Underst 61:154–170
4. Cheong H-B (2000) Double Fourier series on a sphere: applications to elliptic and vorticity equations. J Comput Phys 157:327–349
5. Cheong H-B (2000) Application of double Fourier series to the shallow-water equations on a sphere. J Comput Phys 165:261–287
6. Cohen-Tannoudji C, Diu B, Lalo F (1977) Quantum mechanics. Wiley, New York
7. Driscoll JR, Healy DM Jr (1994) Computing Fourier transforms and convolutions on the 2-sphere. Adv Appl Math 15:202–250
8. Ertürk S, Dennis TJ (1997) 3D model representation using spherical harmonics. Electron Lett 33:951–952
9. Healy D Jr, Rockmore D, Kostelec P, Moore S (2003) FFTs for the 2-sphere—improvements and variations. J Fourier Anal Appl 9:341–385
10. Li J (2002) 3D shape modeling: registration, segmentation, and reconstruction. PhD thesis, Dept. of EECS, Univ. of Michigan, Ann Arbor, 48109-2122
11. Li J, Hero AO (2004) A fast spectral method for active 3D shape reconstruction. J Math Imaging Vis 20:73–87
12. Orszag SA (1974) Fourier series on spheres. Mon Weather Rev 102:56–75
13. Saupe D, Vranic DV (2001) 3D model retrieval with spherical harmonics and moments. Proc DAGM. Munich, Germany, pp 392–397
14. Weinberger HF (1965) A first course in partial differential equations. Wiley, New York
15. Yee SYK (1980) Studies on Fourier series on spheres. Mon Weather Rev 108:676–678
16. Yee SYK (1981) Solution of Poisson's equation on a sphere by truncated double Fourier series. Mon Weather Rev 109:501–505